

CFD Modelling of the Fluid Flow Characteristics in an External-Loop Air-Lift Reactor

Joanna Karcz*, Monika Musiał, Marcelina Bitenc, Marek Domański

West Pomeranian University of Technology, Szczecin, Dept. of Chem. Eng., al. Piastow 42, PL-71-065 Szczecin, Poland,
 Joanna.Karcz@zut.edu.pl

Knowledge about hydrodynamics in the external-loop air-lift reactors is the key in equipment design and process optimization. The aim of the study presented in this paper was numerical analysis of the sparger construction influence on the fluid flow characteristics in an external-loop air-lift column. Unsteady simulations of air - water dispersion flow in the reactor were performed using two fluid Euler-Euler numerical approach. Computational grids were created in commercial package ANSYS Workbench 2. ANSYS CFX 13 solver was used for numerical simulations. The Shear Stress Transport model was used for calculation of the turbulent momentum transport in the liquid phase. Results of the numerical simulation have been worked out in the form of the axial and radial distributions and contours of the gas hold-up, fluid velocity fields, kinetic energy of turbulence and its dissipation rate in the air-lift reactor.

1. Introduction

The increase of the air-lift reactor popularity is reflected in the applying of these devices in various industries. They are used in fermentation processes involving fungi, bacteria, cell culture, as well as aerobic treatment of wastewater. Simple construction of this reactor can be easily adapted to the needs of a given process. The energy is introduced into the system with the gas stream. The air-lift column is characterized by high efficiency in the large range of flow rates and the absence of regions of high shear stress. Other advantages include good gas dispersion, high transfer performance and low costs (Chisti, 1989). Recently, experimental and numerical methods are used for understanding behaviour of the flow in the air-lift reactors. Numerical calculations of two-phase flow for the internal-loop air-lift column concerned such problems as: distributions of gas bubbles (Blažej et al. (2004), Šimčík et al. (2011), Huang et al. (2007), fields of fluid flow (Huang et al. (2010), Keshavarz et al. (2011)), profiles of turbulence kinetic energy (Luo et al. (2011) and optimisation of column dimensions (Hekmat et al. (2010)). However, CFD simulations of two-phase flow in external-loop air-lift reactors are rather limited because the results obtained for such columns were described in few papers only. Hari et al. (2002) simulated both circulation and mixing times. Gas hold-up was modelled by Wang et al. (2004), Dhanasekharan et al. (2005) and Roy et al. (2006). Cao et al. (2009) and Silva et al. (2010) numerically analysed distributions of the gas bubbles in such reactor. Karcz et al. (2011) compared averaged results of numerical computations with the results of experimental study of hydrodynamics in an external-loop air-lift reactor and they stated that both results are consistent.

The aim of the numerical study presented in this paper was to determine the local rate of gas hold-up, fluid velocity, kinetic energy of turbulence and its dissipation in external-loop air-lift column.

2. Range of the simulations

Computational domain, containing scheme of an external-loop air-lift reactor, is shown in Figure 1. Two main parts can be distinguished in this reactor: the riser (R) and the downcomer (D). Inner diameter of the riser was equal to $D_R = 0.1056$ m, and its height was $H_R = 1.932$ m. The downcomer was described by inner diameter $D_D = 0.0464$ m and height $H_D = 1.69$ m. The columns were connected to the top and the

bottom. The distance between the vertical centre lines of both columns was equal to 0.5 m. The riser (R) was divided by the dimensionless axial coordinate h/H in such a way that the bottom of the column had the value of 0.0, and value 1.0 was assigned for the top of the column. In analogous way, this coordinate was ascribed to the downcomer (D). However, it should be noted that total length of the dimensionless axial coordinate of the riser was not equal to analogous coordinate corresponding to the downcomer. The gas sparger had the form of perforated plate with symmetrically placed orifices of a diameter $d_o = 0.002$ m. Numerical computations were carried out for three different numbers of the orifices in the plate, equal to 3, 6 or 12, respectively.

Unstructured grid used for the numerical calculations was generated in ANSYS Workbench 2. It consisted of 668534 or 768287 or 879721 tetrahedral elements for the air-lift reactor equipped with 3 or 6 or 12 orifices in perforated plate, respectively (Figure 2a, 2b, 2c). The numerical calculations were carried out using solver ANSYS CFX 13. Euler – Euler numerical approach was used for unsteady simulations of gas – liquid dispersion within the turbulent range of the fluid flow in the reactor. Air – water system was tested. Gas flow rate was equal to $V_g = 1.21 \times 10^{-4} \text{ m}^3/\text{s}$. The average diameter of bubbles at the inlet was assumed as $d_b = 0.005$ m. The continuous phase was modelled using the Shear Stress Transport turbulence model and Zero Equation model was used for the dispersed phase. The top of the reactor was chosen as an outlet with degassing condition. In order to consider wall influence on the flow option “no slip” for continuous phase and “free slip” constraint for dispersed phase was used in computations.

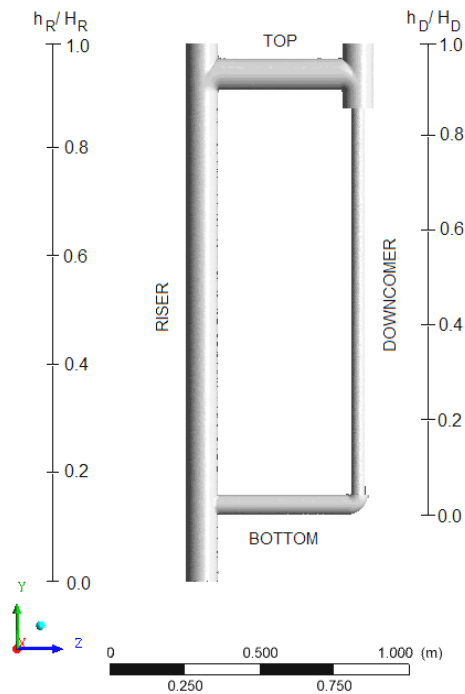


Figure 1: Computational domain of external-loop air-lift reactor

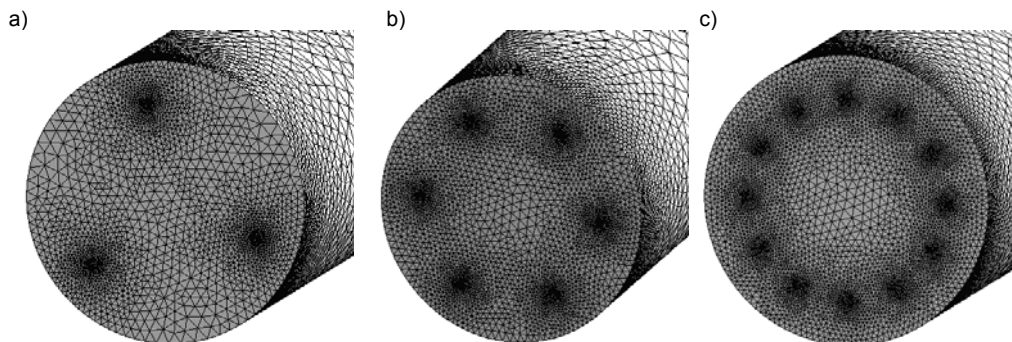


Figure 2: Numerical grid of: a) 3, b) 6, c) 12 orifices in perforated plate

3. Results

The results have been worked out in the form of the contours, as well as radial and axial distributions of the analyzed parameters. Figure 3 shows the contours of gas hold-up ϕ (Figure 3a), turbulence kinetic energy k (Figure 3b), liquid velocity w_c (Figure 3c) and dissipation ε of turbulence kinetic energy (Figure 3d). The results shown in Figure 3 were obtained for external-loop air-lift reactor with six orifices in perforated plate. Computations were carried out for the time step equal to 0.01 s and the gas flow rate $V_g = 1.21 \times 10^{-4} \text{ m}^3/\text{s}$. Figure 4 shows axial distributions of gas hold-up ϕ_R (Figure 4a), turbulence kinetic energy k_R and k_D (Figure 4b, 4c), liquid velocity w_{cR} and w_{cD} (Figure 4d, 4e) and dissipation ε_R and ε_D of turbulence kinetic energy (Figure 4f, 4g) for the riser and the downcomer.

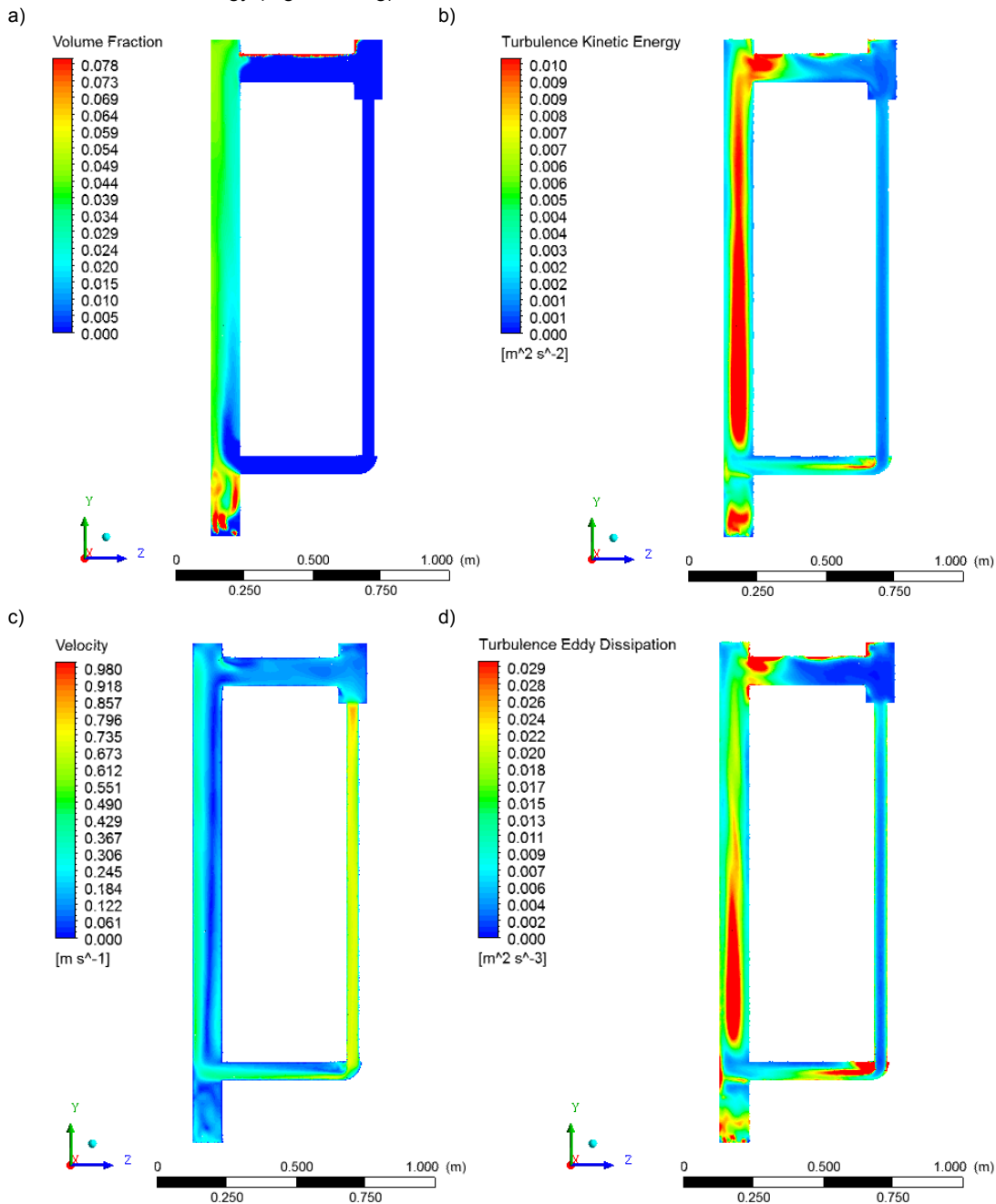


Figure 3: Results of the numerical simulations a) gas hold-up, b) turbulence kinetic energy, c) liquid velocity, d) dissipation of turbulence kinetic energy for the external-loop air-lift reactor with six orifices in perforated plate; gas flow rate $V_g = 1.21 \times 10^{-4} \text{ m}^3/\text{s}$

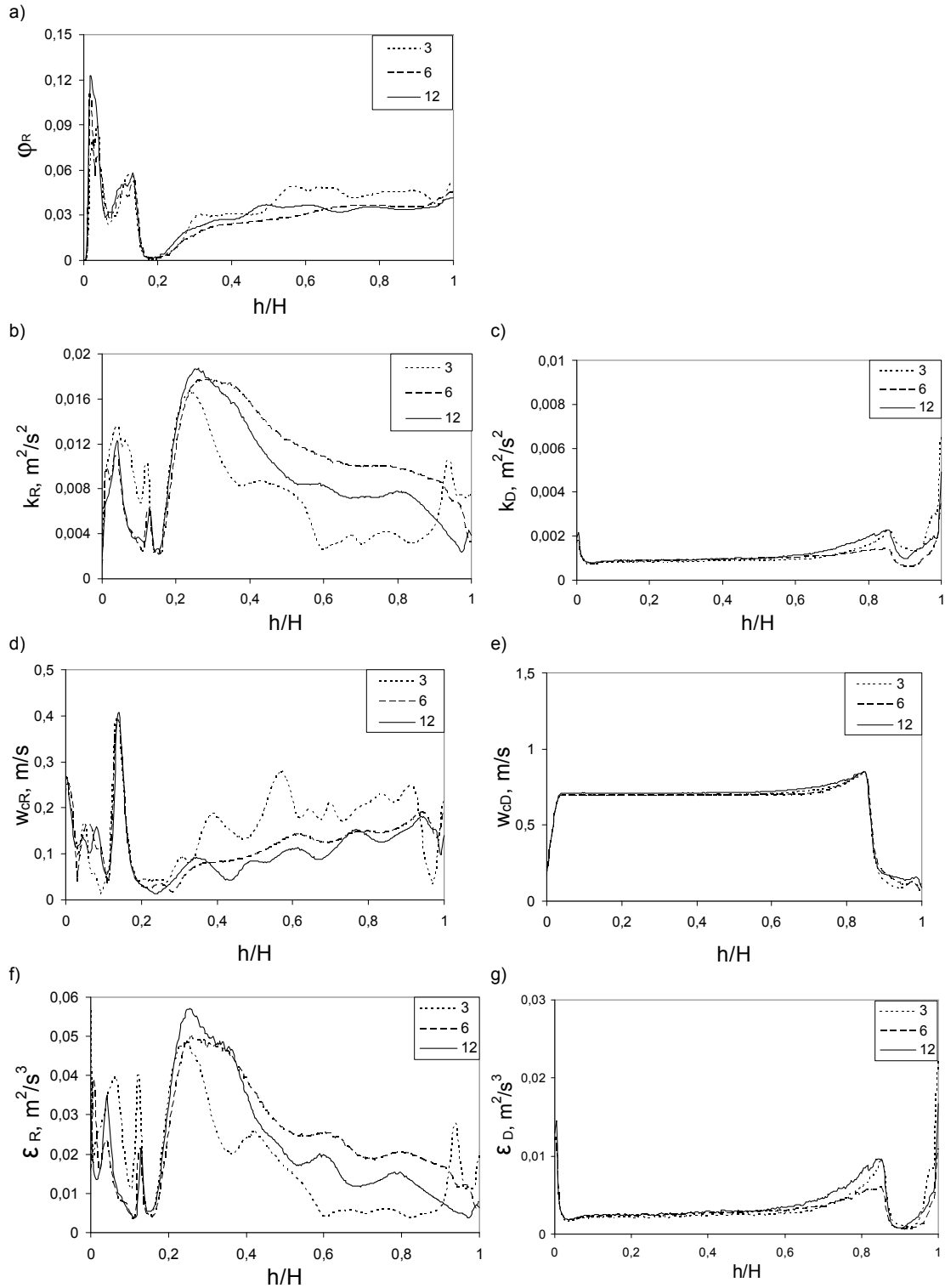


Figure 4: Axial distributions of a) gas hold-up in the riser, b) turbulence kinetic energy in the riser, c) turbulence kinetic energy in the downcomer, d) liquid velocity in the riser, e) liquid velocity in the downcomer, f) dissipation of turbulence kinetic energy in the riser, g) dissipation of turbulence kinetic energy in the downcomer of external-loop air-lift reactor for gas flow rate $V_g = 1.21 \times 10^{-4} m^3/s$; dotted line - three orifices in perforated plate, dashed line - six orifices in perforated plate, solid line - twelve orifices in perforated plate

From Figures 3 and 4 can be seen that, in each case of the number orifices in perforated plate, the highest value of gas hold-up is observed in the location nearby the gas distributor. At the height $h_R/H_R = 0.2$ can be noted a decline of gas hold-up value in the axis of the column due to the recycle stream. It influences the structure of the flow strongly causing displacement upwardly flowing stream in the left direction. The gas hold-up in the downcomer is negligible. Axial distributions of liquid velocity in the reactor indicate the increase of this parameter in the axis of the riser with an increase of the dimensionless axial coordinate. In the downcomer the highest value of the liquid velocity can be observed at narrowing the vertical pipe. The decrease can be noted when the horizontal and vertical tube combined, which is associated with the change in the flow direction. Minimum values of the turbulence kinetic energy and its dissipation can be seen at the level of the connection of the main stream and the recycle stream. It is also noted that the values of the turbulence kinetic energy and its dissipation reach the maximum at the level $h_R/H_R = 0.2$, and then decrease with the increase of the dimensionless axial coordinate h/H . In the downcomer the highest values of turbulence kinetic energy and its dissipation can be noted at the bottom of the downcomer and at the top, where the gas leaves the system causing the motion of liquid surface and thus increase turbulence in the flow.

Based on presented results it was found that the external-loop air-lift column can be divided into several characteristic regions which have an impact on the hydrodynamics. The first region in the riser is the position of the gas distributor ($h_R/H_R \in <0, 0.2>$) where gas is continuously fed to the column. Going up the riser, $h_R/H_R \in (0.2, 0.4>$, the recycle stream of fluid flowing from the lower horizontal pipe affects the flow. In the central part of the riser ($h_R/H_R \in (0.4, 0.9>$), the flow parameters are at least dependent on design of the column. The separation zone ($h_R/H_R \in (0.9, 1>$) is characteristic of the observed liquid velocity, which takes lower values due to the change in flow direction. In the downcomer there are also some specific areas, firstly, the connection of horizontal and vertical pipe ($h_D/H_D \in <0, 0.05>$). In this zone liquid deceleration is caused by changes in flow direction. The central part of the downcomer ($h_D/H_D \in (0.05, 0.6>$) is characterized by a constant liquid velocity. In the region located higher, $h_D/H_D \in (0.6, 0.85>$, the reduction of set up over the cross-sectional pipe area affects the non-linear change in liquid velocity. The liquid velocity decreases to a minimum and is mainly dependent on movement of gas bubbles leaving the reactor in the region $h_D/H_D \in <0.85, 1>$ where the horizontal and vertical pipes combined.

Table 1 shows the comparison of the mean values of the gas hold-up in the riser, the liquid velocity in the riser and in the downcomer. These results are related to the values obtained for the radial distributions of a given column height. The highest values of the gas hold-up received for the construction with 3 orifices in the perforated plate. The values obtained for the liquid velocity in the downcomer were much higher than in the riser in each case, which was caused by the narrowing of the vertical pipe and the gravity. Near the connection of the lower horizontal pipe, liquid velocity received lower values due to the deceleration of the liquid by changing the flow direction.

Table 1: Comparison of mean values of the gas hold-up in the riser, the liquid velocity in the riser and in the downcomer

| number of orifices | 3 | | | 6 | | | 12 | | |
|--------------------------|-------------|--------------|--------------|-------------|--------------|--------------|-------------|--------------|--------------|
| | φ_R | w_{cR} m/s | w_{cD} m/s | φ_R | w_{cR} m/s | w_{cD} m/s | φ_R | w_{cR} m/s | w_{cD} m/s |
| level h/H | | | | | | | | | |
| 0.0 | 0.021 | 0.221 | 0.250 | 0.027 | 0.200 | 0.219 | 0.036 | 0.202 | 0.239 |
| 0.2 | 0.020 | 0.191 | 0.675 | 0.017 | 0.187 | 0.671 | 0.017 | 0.199 | 0.691 |
| 0.4 | 0.036 | 0.146 | 0.676 | 0.028 | 0.176 | 0.672 | 0.030 | 0.169 | 0.693 |
| 0.6 | 0.040 | 0.174 | 0.680 | 0.031 | 0.168 | 0.672 | 0.037 | 0.158 | 0.698 |
| 0.8 | 0.035 | 0.160 | 0.708 | 0.034 | 0.167 | 0.703 | 0.034 | 0.156 | 0.720 |
| 1.0 | 0.045 | 0.158 | 0.070 | 0.043 | 0.153 | 0.106 | 0.039 | 0.112 | 0.099 |

4. Conclusions

Advanced numerical simulations enable to predict the local hydrodynamic parameters, allowing for in-depth knowledge of the nature of the liquid - gas dispersion. The SST model is acceptable in terms of accuracy of the calculations and computing power input. Within the range of the computations performed for the external-loop air-lift reactor, it can be stated unequivocal impact of the orifices numbers in gas sparger (shaped in the form of perforated plate) on the simulation results.

References

- Ansys CFX, Release 10.0: Modelling, 2005, Ed. Ansys Europe Ltd.
- Blažej M., Cartland Glover G.M., Generalis S.C., Markoš J., 2004, Gas-liquid simulation of an airlift bubble column reactor, *Chemical Engineering and Processing*, 43, 137–144
- Cao C., Zhao L., Xu D., Geng Q., Guo Q., 2009, Investigation into bubble size distribution and transient evolution in the sparger region of gas-liquid external loop airlift reactors, *Ind. Eng. Chem. Res.*, 48, 5824–5832
- Chisti M.Y., 1989, *Airlift bioreactors*. Elsevier Applied Science, London and New York
- Dhanasekharan K. M., Sanyal J., Jain A., Haidari A., 2005, A generalized approach to model oxygen transfer in bioreactors using population balances and computational fluid dynamics, *Chemical Engineering Science*, 60, 213–218
- Hari M., Tan R. B. H., 2002, A dynamical systems approach to mixing in circulating flows, *Chem. Eng. Technol.*, 25, 811–818
- Hekmat A., Amooghin A.E., Moraveji M.K., 2010, CFD simulation of gas-liquid flow behaviour in an air-lift reactor: determination of the optimum distance of the draft tube, *Simulation Modelling Practice and Theory*, 18, 927–945
- Huang Q., Yang C., Yu G., Mao Z-S., 2007, 3-D simulations of an internal airlift loop reactor using a steady two-fluid model, *Chem. Eng. Technol.*, 30, 870–879
- Huang Q., Yang C., Yu G., Mao Z-S., 2010, CFD simulation of hydrodynamics and mass transfer in an internal airlift loop reactor using a steady two-fluid model, *Chemical Engineering Science*, 65, 5527–5536
- Karcz J., Bitenc M., Domański M., Kacperski Ł., 2011, Numerical study of hydrodynamics in an external-loop air-lift reactor, *Chemical Engineering Transactions*, 24, 1399-1404
- Keshavarz Moraveji M., Sajjadi B., Jafarkhani M., Davarnejad R., 2011, Experimental investigation and CFD simulation of turbulence effect on hydrodynamic and mass transfer in a packed bed airlift internal loop reactor, *International Communications in Heat and Mass Transfer*, 38, 518–524
- Luo H-P, Al-Dahhan H. M., 2011, Verification and validation of CFD simulations for local flow dynamics in a draft tube airlift bioreactor, *Chemical Engineering Science*, 66, 907–923
- Roy S., Dhotre M.T., Joshi J.B., 2006, CFD simulation of flow and axial dispersion in external loop airlift reactor, *Chemical Engineering Research and Design*, 84, 677–690
- Silva M. K., d'Avila M A., Mori M., 2010, CFD modelling of a bubble column with an external loop in the heterogeneous regime, *The Canadian Journal of Chemical Engineering*, 89, 671–681
- Šimčik M., Mota A., Ruzicka M. C., Vicente A., Teixeira J., 2011, CFD simulation and experimental measurement of gas hold-up and liquid interstitial velocity in internal loop airlift reactor, *Chemical Engineering Science*, 66, 3268–3279
- Wang T., Wang J., Jin Y., 2004, Experimental study and CFD simulation of hydrodynamic behaviours in an external loop airlift slurry reactor, *The Canadian Journal of Chemical Engineering*, 82, 1183–1190